1 # Reconstruction of mass balance and firn stratigraphy during the

2 # 1996-2011 warm period at high-altitude on Mt. Ortles, Eastern

3 # Alps: a comparison of modelled and ice core results

4

5 Luca Carturan[1], Alexander C. Ihle[2,3], Federico Cazorzi[4], Tiziana Lazzarina Zendrini[1], Fabrizio De

6 Blasi[1,5], Giancarlo Dalla Fontana[1], Giuliano Dreossi[6], Daniela Festi[7], Bryan Mark[3], Klaus Dieter

7 Oeggl[8], Roberto Seppi[9], Barbara Stenni[6], Paolo Gabrielli[10]

8

9 [1]Department of Land, Environment, Agriculture and Forestry, University of Padua, Legnaro, Italy

10 [2]Department of Earth and Environmental Sciences, University of Rochester, Rochester, USA

11 [3]Department of Geography and Byrd Polar and Climate Research Institute, Ohio State University, Columbus, USA

12 [4]Department of Agricultural, Food, Environmental and Animal Sciences, University of Udine, Udine, Italy

13 [5]Consiglio Nazionale delle Ricerche - Istituto di Scienze Polari, c/o Ca' Foscari University of Venice, Venice, Italy

14 [6]Department of Environmental Sciences, Informatics and Statistics, Ca' Foscari University of Venice, Venice, Italy

15 [7]GeoSphere Austria, Department of Geoanalytics and Reference Collections, Vienna, Austria

16 [8]Department of Botany, University of Innsbruck, Innsbruck, Austria

17 [9]Department of Earth and Environmental Sciences, Pavia, Italy

18 [10]Italian Glaciological Committee, Torino, Italy

19 *Correspondence to:* Luca Carturan (luca.carturan@unipd.it)

20

21 **Abstract**

22 Paleoclimatic glacial archives in low-latitude mountain regions are increasingly affected by melt, which leads to heavy

23 percolation and can remove snow and firn accumulated across months, seasons or even years. Proxy system models, used

24 for improved interpretation of glacial proxies and paleoclimatic reconstructions, generally do not account for melt because

25 they are optimized for sites where snow layer removal by melting is negligible. In this paper, we present a mass balance

26 model applied to the Mt. Ortles drilling site, at 3859 m a.s.l. in the Eastern Italian Alps, with the aim of building a pseudo

27 proxy of atmospheric conditions during the formation of snow layers survived to ablation. This pseudo proxy is useful

28 for improved dating and environmental interpretation of firn layers (<15 m depth), affected by significant melt in the

29 period 1996-2011, which includes the extremely warm summer 2003. Here we show that the model significantly improves

30   the interpretation of the firn stratigraphy. This is fundamental for detecting melted layers and for refining the dating of

31   the core based on traditional annual layer counting of stable isotope and pollen seasonal oscillations.

32

1 Introduction

34   Atmospheric warming is threatening paleoclimatic glacial archives, particularly those located in low-latitude mountain

35   areas (e.g. Gabrielli et al., 2010; Huber et al., 2024). When compared to polar ice sheets in Greenland and Antarctica,

36   these glaciers are now altitudinally closer to their lower limits of formation and preservation.

37   Long before their complete disappearance, glacial archives are affected by post-depositional processes caused by

38   increasing temperature, which modifies and ultimately overprints their paleoclimatic signals. Increasing frequency and

39   intensity of surface melt events lead to snow/firn layer mass loss and heavy percolation of meltwater through the firn.

40   This obliterates part of the glacial archive and smooths or dislocates intra/inter-annual variations of chemical impurities

41   of interest for paleoclimatic reconstructions (Dietermann & Weiller, 2013; Gabrielli et al., 2010; Hashimoto et al., 2005;

42   Lee, 2014; Moran et al., 2011; Moser et al., 2024, Thompson et a., 2011, 2021; Unnikrishna et al., 2002).

43   It is unclear how extreme melt events, such as the summer 2003 heat wave in the European Alps (Zappa and Kan, 2007;

44   García-Herrera et al., 2010), affect the preservation of ice core archives. This kind of events may significantly change the

45   original isotopic record, melting the snow accumulated over several months or years (Gabrielli et al. 2010). In addition it

46   is unknown whether such extreme events may relocate less mobile impurities such as pollens or black carbon, as their

47   annual cycle is generally preserved under melting conditions, and are therefore used for ice core dating (Pavlova et al.,

48   2015; Festi et al., 2021; Takeuchi et al., 2019; Moser et al., 2024).

49   Atmospheric warming also affects snow water content and its metamorphism, which control snow redistribution by wind.

50   For this reason, snow drifting is expected to be most effective for cold and dry snow and less so for wet snow and melt-

51   freeze crusts (Haeberli and Alean, 1985, Li and Pomeroy, 1997; He and Ohara, 2017). This process can influence the

52   snow accumulation rate and the formation/preservation of the isotopic record and other chemical signals (Bohleber, 2019;

53   Bohleber et al., 2013; Nakazawa et al., 2005). This adds complexity to dating and interpretation of ice cores archives,

54   particularly for those retrieved at high elevation in non-polar glacierized areas subjected to significant snow melt and

55   wind redistribution. In this case, annual layer counting is difficult because surface melt and/or wind redistribution remove

56   snow layers formed across months or seasons (Neff et al., 2012). As these processes are typical of these mid-to-low

57   latitude regions and are part of the glacial archive's response to climate change, their understanding is a fundamental

58   prerequisite for paleoclimatic reconstructions.

59   Glacier mass balance modelling at ice core drilling sites is useful to reconstruct the formation and preservation of glacial

60   archives and their ongoing changes due to atmospheric warming. Mass balance models can provide information on the

61   amount of surface melt, meltwater percolation, and magnitude of snow accumulation by precipitation and wind drifting.

62   Overall, these model outputs can help to detect and characterize events linked to i) snow layer formation, ii) snow layer

63   removal, and iii) snow layer modifications (e.g. warming, wetting, refreezing). This information may also help in

64   detecting deviations of ice core proxies from the generally assumed linear, univariate recording of local temperature

65   (Evans et al., 2013). In fact, this assumption may not hold in the long term, particularly under extreme conditions such as

66   current or past warm climatic phases, especially at sensitive locations such as mid-to-low-latitude glacierized areas.

67   Proxy system models (models that describe the processes by which environmental conditions are recorded in a proxy

68   archive) linked to isotope-enabled atmospheric general circulation models (models that describe isotopic variations in

69   precipitation for a geographic area) are increasingly used to constrain ice core-based paleoclimatic reconstructions and

70   for complementing interpretations based solely on statistical analyses (Evans et al., 2013). Proxy system models of various

71   complexities were developed for ice core proxy interpretation (e.g., Brönnimann et al., 2013; Hurley et al., 2016; Okazaki

72   and Yoshimura, 2019). These models reconstruct how stable water isotopes are recorded in ice core archives, generating

73   a pseudo proxy that is compared to the actual proxy, to complement it and improve its paleoclimatic interpretation. For

74   example, the possibility to disentangle different processes (temperature, intermittency of precipitation, diffusion)

75   affecting the isotopic records to extract the "real" climatic signal, by using a so called "virtual" ice core, has been studied

76   for Antarctica (Laepple et al, 2018).

77   These models are optimized for sites where snow layer removal by melting is negligible and snow redistribution can be

78   accounted for by stacking ice core records from adjacent sites located in the same area (e.g., Ekaykin and Lipenkov,

79   2009). Additionally, models implicitly assume stationarity (or negligible variations) of snow redistribution, melt, and

80   meltwater percolation. This is not always the case, particularly for low-latitude drilling sites where cold climatic phases

81   that are favourable for ice core proxy formation and preservation alternate with warm climatic phases that are

82   unfavourable.

83   The Mt. Ortles drilling site, at 3859 m a.s.l. in the Eastern Alps (Italy), has been characterised by a rapid warming of the

84   firn and snow layers since the 1980s. Atmospheric warming is seriously threatening this paleoclimatic archive (Gabrielli

85   et al., 2010) due to the increasing length and intensity of the ablation season, causing significant surface melt and

86   meltwater percolation. In summer the firn layer is now entirely isothermal at the pressure melting point (Carturan et al.,

87   2023). The ice below the firn-ice transition (30 m depth) is still cold, with temperature down to -2.8°C close to the bedrock

88   in 2011 (Gabrielli et al., 2012). This shows that conditions favourable for glacial archive formation and preservation still

89   exist on Mt. Ortles. However, the relatively low elevation of this ice core-drilling site makes it sensitive to climatic

90   fluctuations and particularly vulnerable to non-linear processes controlled by snowmelt, snow metamorphism, and wind

91   redistribution.

92   In this paper, we present a model-based reconstruction of the mass balance history and firn stratigraphy at the Mt. Ortles

93   drilling site in the 1996-2011 warm period, including the extremely warm summer 2003 (García-Herrera et al., 2010).

94   The aim is understanding the effects of exceptionally warm periods on glacier mass balance and the ice core paleoclimatic

95   archive. Specifically, the mass balance model used in this work was implemented to: i) model the formation of snow and

96   firn layers, ii) identify snow layers removed by ablation, iii) reconstruct the air temperature during the formation of snow

97   layers that survived successive ablation. This latter is a pseudo proxy that we ultimately compare to stable water isotopes

98   retrieved in the firn layers of the same period, to revise the dating of the firn portion of the Mt. Ortles ice core.

99

100   **2 Study area**

101   Mount Ortles (3905 m a.s.l.), in the Ortles-Cevedale Mountain Group, is the highest summit of South Tyrol in the Eastern

102   European Alps. Its northern flank is covered by the Alto dell'Ortles Glacier (Oberer Ortlerferner-Vedretta Alta

103   dell'Ortles), which extends over an area of 1.06 km^2 (2017) and ranges in elevation between 3018 and 3905 m a.s.l. (Fig.

104   1). The ice core drilling site is located at 3859 m a.s.l. in the upper accumulation area, close to a saddle (Figs. 1 and 2).

105 The glacier's maximum thickness at the drilling site is about 75 meters (Gabrielli et al., 2012) and the ice is ~7-kyr old at
106 the glacier base (Gabrielli et al., 2016). In this zone the glacier is polythermal, with temperate firn and cold ice underneath
107 the firn-ice transition, at ~30 m depth (Gabrielli et al., 2012). The Ortles ice archive is one of the only two cold ice archives
108 found in the eastern Alps, with the other being the nearby Weißseespitze (Cima del Lago Bianco) summit ice dome
109 (Bohleber et al., 2020; Gabrielli et al., 2012).

110 The local climate is characterized by a continental regime, with a mean annual precipitation in the period 1981-2010 of
111 800–950 mm yr^{-1} at the valley floor in Solda (Adler, 2015). The annual precipitation on the top of Mt. Ortles is estimated
112 to range between 1300 and 1400 mm, using in-situ mass balance observations performed between 2009 and 2016,
113 (Carturan et al., 2023). This precipitation estimate is subject to large spatial variability due to the influence of wind on
114 snow accumulation and redistribution.

115 The mean annual air temperature at 3850 m a.s.l. on Mt. Ortles is about -9°C. On the glaciers of the Ortles-Cevedale
116 Group the snow cover follows a typical annual cycle, with accumulation prevailing between October and May, and
117 ablation between June and September. Due to the high elevation of the drilling site, snowfalls are also frequent during
118 summer. There is high interannual variability in the amount and duration of ablation events, which occur primarily during
119 heatwaves. Liquid precipitation is very rare, although some rain events have been recorded at the drilling site elevation
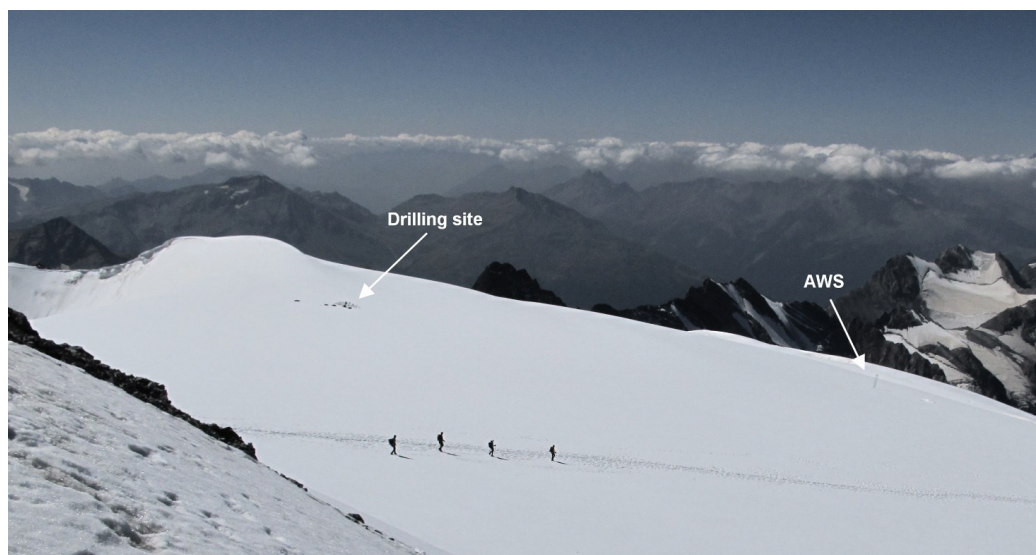120 over the past 15 years (Carturan et al., 2023).

121

122

123

124
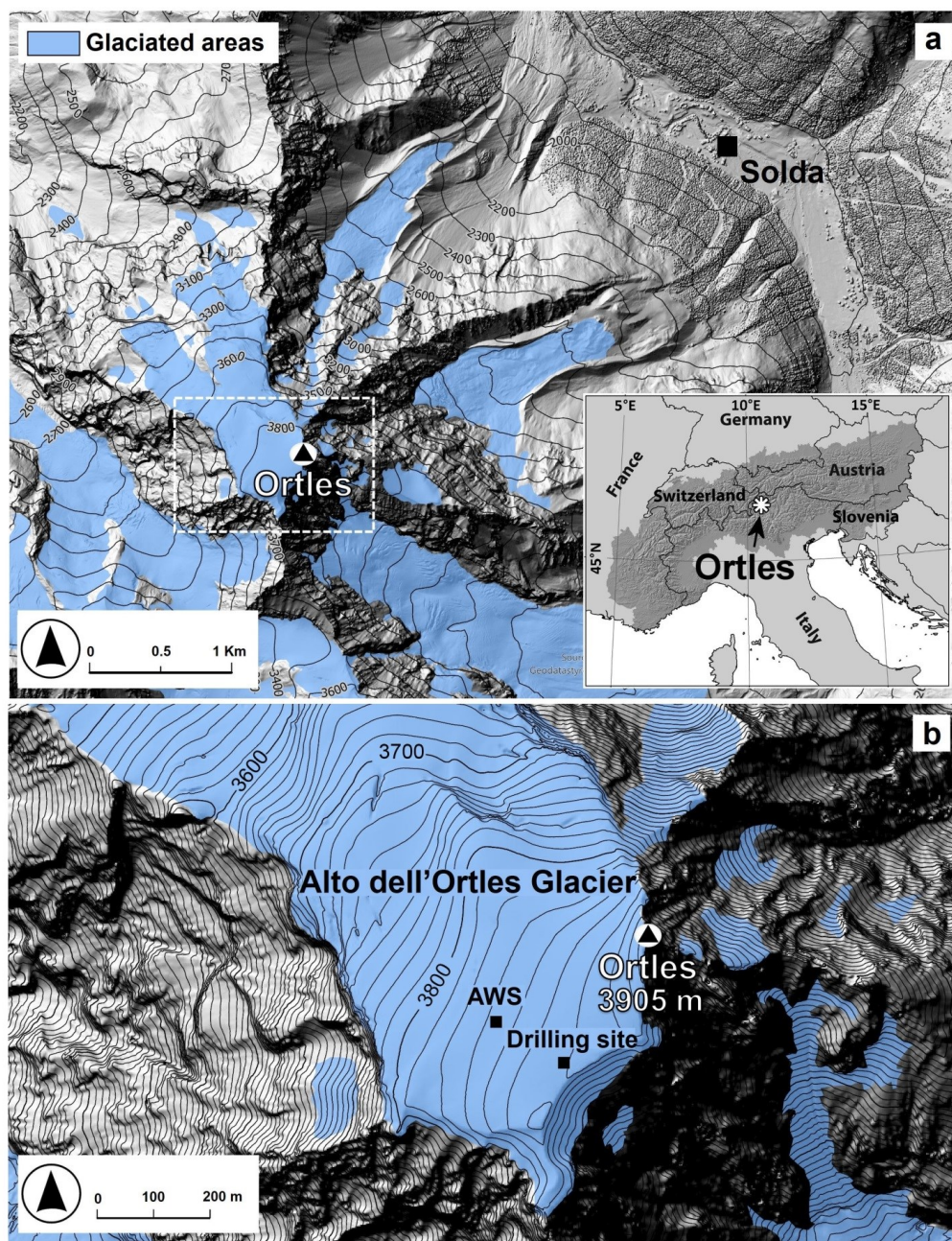
Figure 1: Location of the drilling site and automatic weather station (AWS) on Mt. Ortles. The background hill-shaded DEM (2017 lidar survey) is from http://geocatalogo.retecivica.bz.it/ (last access: 10 January 2025) (Agenzia per la Protezione civile, Autonomous Province of Bolzano).

130

131

Figure 2: Photo of the upper accumulation area of Alto dell'Ortles Glacier taken from the summit of Mt. Ortles on 31
August 2015.

135

3 Methods

3.1 Ice core drilling operations

Four ice cores were drilled within 20 m of each other during September and October 2011 on a small col on the Alto
dell'Ortles Glacier, between the summit of Mt. Ortles and the Vorgipfel (UTM zone 32T, 618364 m easting, 5151531 m
northing, 3859 m altitude). In this study, we focus on core 1, which reached 73.53 m depth, because it is the only one for
which both complete isotope and pollen records are available. (Gabrielli et al., 2016).

142

3.2 Ice core analyses

Ortles core 1 was cut in a cold room (-20°C) at the Ca' Foscari University of Venice (Italy). Analysis resolution increased
with increasing depth, from 9 cm per sample (0-5 m depth), to 2 cm per sample (from 49 m to bottom).

Oxygen and hydrogen isotopic composition analyses were performed with two analytical methods. One method uses the
well-established CO_2-H_2/water equilibration technique (Horita et al., 1989) which couples an automatic equilibration
device (Finnigan MAT HDO 1086) with an isotope ratio mass spectrometer (Thermo-Fisher Delta Plus Advantage). Five
ml of water were used and the analytical uncertainty for $\delta^{18}O$ and δD was ± 0.05‰ (1σ) and ±0.7‰ (1σ), respectively.
The other method was the wavelength-scanned cavity ring-down spectroscopy technique (PICARRO model L1102-i).
Since the injections of water samples can be affected by between-sample memory effects (Penna et al., 2012), samples

152 were injected (2 □l) 8 times and results were filtered using an outlier test. The analytical uncertainty for $\delta^{18}O$ and δD was

153 ± 0.10‰ (1σ) and ±0.5‰ (1σ), respectively. In each analysis run, two internal standards (periodically calibrated against

154 the IAEA international standards V-SMOW2 and SLAP2) were analysed along with the samples, and used for building

155 a calibration curve. The results were reported in the usual delta notation (δ) and expressed as per mil (‰).

156 Pollen analyses were performed at the Institute of Botany of the University of Innsbruck. Aliquots of up to 35 ml water

157 (depending on sample resolution) were used. Each sample was decontaminated with cold distilled water and the volume

158 of the water resulting from the ice melting was measured. Samples were processed with acetolysis (Erdtman, 1960) and

159 the pollen content was concentrated by hydro-extraction (centrifugation) and then prepared in glycerine slides (Faegri

160 and Iversen, 1989). The complete pollen content of the samples has been identified and quantified, as detailed in Festi et

161 al. (2015). For each sample, pollen concentration (grains ml^{-1}) was calculated. To detect the seasonality a principal

162 component analysis (PCA) has been performed on the pollen dataset according to the methodology developed in Festi et

163 al (2015). Three principal components indicative of the three main flowering seasons (spring, early summer and late

164 summer) were hereby extracted and are presented graphically. Peaks in component score values of a specific PC reflect

165 a pollen content characteristic predominant in the season corresponding to that particular PC. This method was applied to

166 the dataset as previous studies showed that the Ortles glacier pollen assemblages are representative for the regional

167 vegetation and comparable with airborne assemblages recorded at the nearby aerobiological stations (Festi et al., 2015).

168

3.3 Mass balance observations

170 Seasonal and annual glacier mass balances were measured at the drilling site and at the automatic weather station site

171 (Section 3.4., Figs. 1 and 2) from June 2009 to September 2014. Winter balance observations were typically carried out

172 in June/early July before the onset of melt, while summer/annual balance were performed in late August/early September

173 at the end of the melt season.

174 Observations consisted of snow depth soundings with a metal probe in the surroundings of the two sites, and of snow/firn

175 density measurements inside snow pits dug to the previous summer surface. Detailed snow stratigraphic observations

176 were carried out at shaded snow pit walls, comprising snow/firn temperature, hardness, grain type and size, location of

177 ice lenses and dust layers (e.g. Gabrielli et al. 2010). Stratigraphic observations were helpful in recognising summer

178 surfaces both in snow pits and during snow depth soundings. Density measurements were used to convert snow depths

179 into water equivalent depths.

180

3.4 Meteorological observations

182 The meteorological data used in this work are from an automatic weather station (AWS) located in the valley floor village

183 of Solda (Fig. 1, 1907 m a.s.l.) about 4.5 km northeast of Mt. Ortles. This AWS is part of the network of AWSs operated

184 by the Hydrological Office of the Autonomous Province of Bolzano (meteo.provincia.bz.it).

185 To collect additional meteorological observations, the Ortles paleoclimatological project (ortles.org) installed an AWS

186 close to the drilling site in October 2011 (Figs. 1 and 2). The AWS worked until June 2015 and was equipped with air

187 temperature, relative humidity, wind speed and direction, shortwave and longwave incoming and outgoing radiation, and

188 snow depth sensors. Details on Ortles AWS instrumentation and datasets are provided in Carturan et al. (2023).

189

3.5 Mass balance modelling

191 The mass balance model used in this study is EISModel, an energy-index model implemented for mass balance
192 computations on glaciers and seasonal snowpacks. The model in its original version is described by Cazorzi and Dalla
193 Fontana (1996), followed by Carturan et al. (2012a) who presented an advanced version for glacial environments. The
194 model was further developed for applications on Mt. Ortles, as detailed in Festi et al. (2017). In this section, we recall the
195 main features of EISModel and describe how it was applied to the study area.

196 The model was applied at hourly time steps. Snow accumulation was calculated from the hourly precipitation data of the
197 Solda AWS, validated against other neighbouring AWSs (Madriccio at 2825m and Cima Beltovo at 3328 m) and corrected
198 for gauge under-catch errors using the method proposed by Carturan et al. (2012b). Precipitation was extrapolated to the
199 elevation of the study site using a precipitation linear increase factor (PLIF, % km^{-1}), which is a lumped parameter that
200 accounts for the vertical increase of precipitation with elevation, preferential deposition, and erosion by wind.
201 Precipitation was classified as liquid or solid depending on the hourly air temperature, which is extrapolated from the
202 Solda AWS using monthly-variable temperature lapse-rates calculated between the Solda and Ortles AWSs.

203 Hourly melt rates were calculated using the following equation:

204 $$MLT_t = RTMF \cdot CSR_t (1 - \alpha_t) \cdot T_t \tag{1}$$

205 where $RTMF$ is the radiation–temperature melt factor (mm h^{-1} °C^{-1} W^{-1} m^2), CSR_t (W m^{-2}) is the clear-sky shortwave
206 radiation computed hourly based on the local topography, T_t is the air temperature, and α_t is the surface albedo calculated
207 in function of cumulative positive T_t (Carturan et al., 2012a).

208 The RTMF and PLIF parameters were initially calibrated at the Ortles AWS site using mass balance observations carried
209 out between 2009 and 2014. For a more robust calibration, we extended backwards to 2005 the mass balance observations,
210 using pollen dating of firn layers (Festi et al., 2017). We preferred to initially calibrate the model at the AWS site, rather
211 than at the drilling site, because field observations are more extensive and consistent at that site. The PLIF parameter was
212 then recalibrated at the drilling site, to account for lower snow accumulation. Finally, the model was applied to reconstruct
213 the cumulated mass balance in the period from September 1996 to September 2011.

214 The pseudo proxy to be compared to stable water isotopes in firn cores was obtained by calculating the air temperature
215 during the formation of snow layers that survived to ablation. We define as a snow layer the water equivalent of snow
216 that accumulates at the surface in one hour. For each snow layer surviving the following ablation, the model provided its
217 time and date of formation and the air temperature during its deposition, which is a variable named SLFT (snow layer
218 formation temperature). The model did not explicitly simulate snow removal by wind drift, which was computed
219 statistically by means of the PLIF multiplicative factor. The water equivalent thickness of each snow layer composing the
220 final snowpack was finally adjusted to account for layer thinning with depth, using the Nye (1963) ice flow model
221 (similarly to, for example, Eichler et al. (2000) and Brönnimann et al. (2013)).

222

4 Results

4.1 Model calibration

225   The calibrated values of the two parameters RTMF and PLIF optimized at the AWS site on Mt. Ortles were 10^{-3} mm h^{-1}

226   °C^{-1} W^{-1} m^2 and 15 % km^{-1}, respectively. At the ice core drilling site (located 200 m uphill of the AWS), the PLIF was

227   recalibrated to 8 % km^{-1} to account for lower snow accumulation, probably due to higher wind erosion.

228   The model performance, expressed by the root mean square error (RMSE), is better for summer balance compared to

229   winter balance, and in closer agreement with observations at the AWS site, compared to the drilling site (Fig. 3). This

230   behaviour was expected because the drilling site is more exposed to wind action and likely experiences stronger snow

231   redistribution, particularly during winter. These results are similar to previous applications of EISModel on Mt. Ortles

232   (Festi et al., 2017).

233
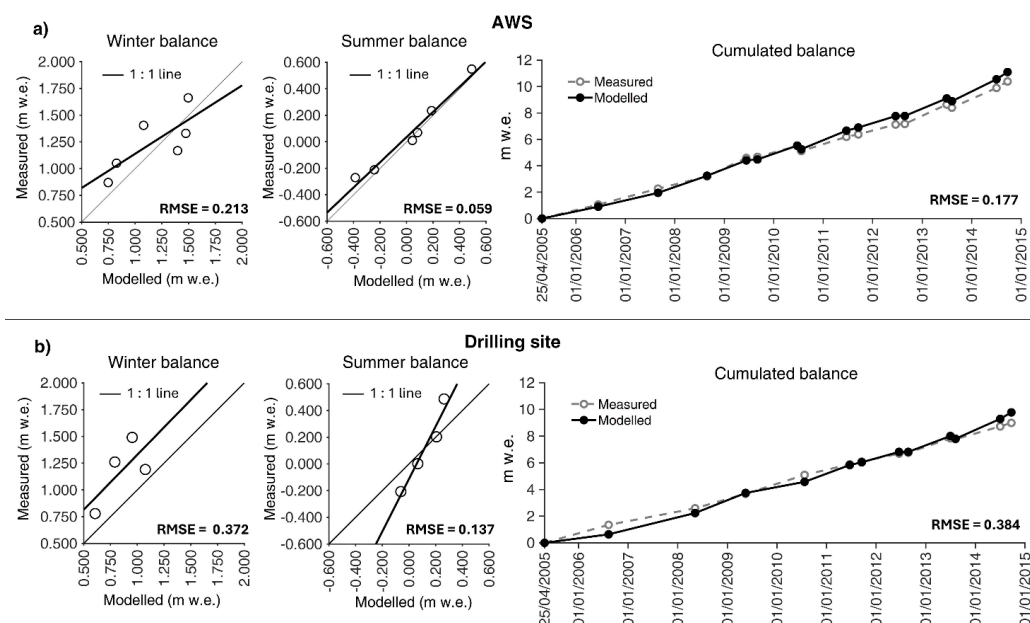
235   Figure 3: EISModel calibration results obtained on Mt. Ortles at a) the AWS site and b) the drilling site, for winter,

236   summer and cumulated mass balance, in the period (2005-2014).

237

238   **4.2 Mass balance behaviour**

239   Based on EISModel calculations, 21.4 and 18.9 m w.e. accumulated from September 1996 to September 2014 at the AWS

240   and ice core drilling sites, respectively (Fig. 4). Accordingly, the accumulation rate averaged 1.18 m w.e. y^{-1} at the AWS

241   site and 1.05 m w.e. y^{-1} at the drilling site. The accumulation rate was smaller between 1997 and 1998 and between 2003

242   and 2008, and increased in the periods between 1999 and 2002 and after 2008 (Figs. 4 and 5).
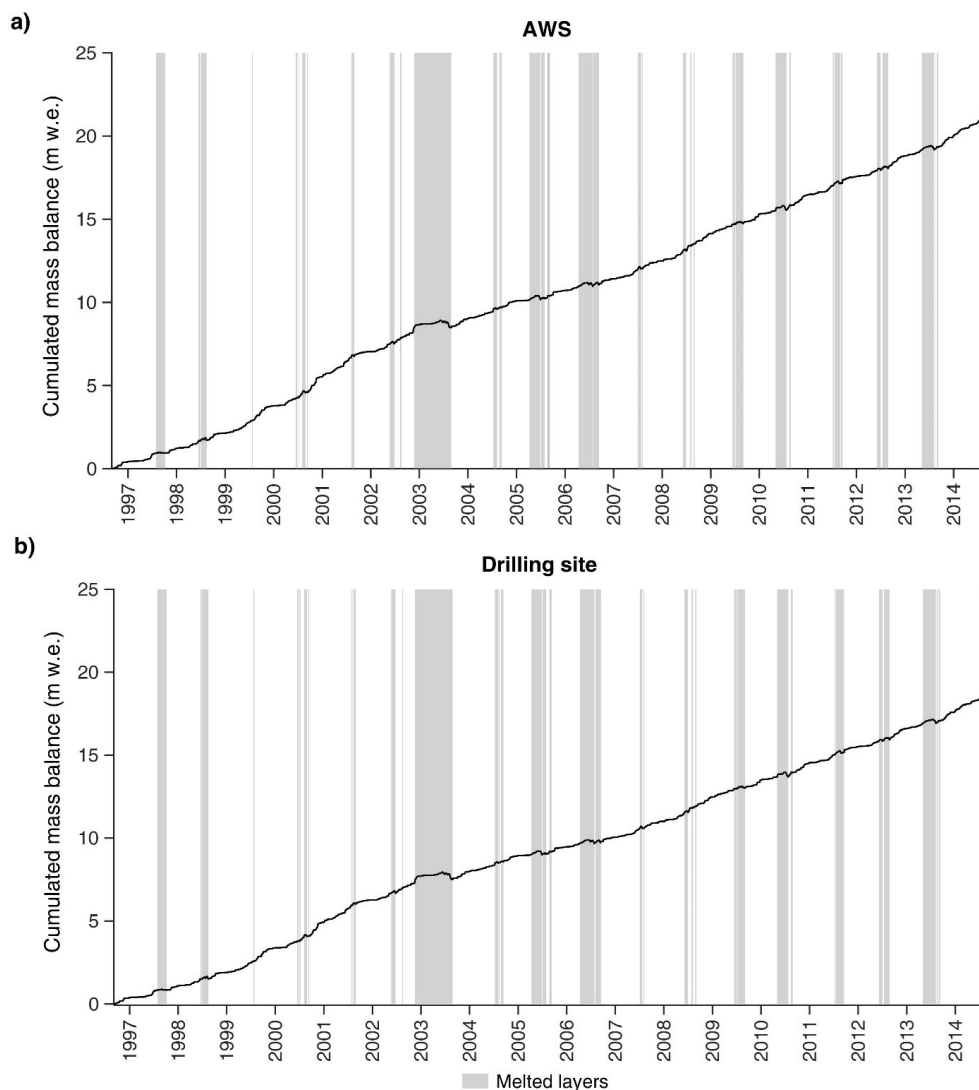
Figure 4: Cumulated mass balance modelled by EISModel at a) the AWS site and b) the drilling site. The vertical bars represent periods of snow accumulation that were removed by melt: large bars mean melting of snow accumulated over long periods (several months), whereas thin bars mean melt of snow accumulated over short periods.
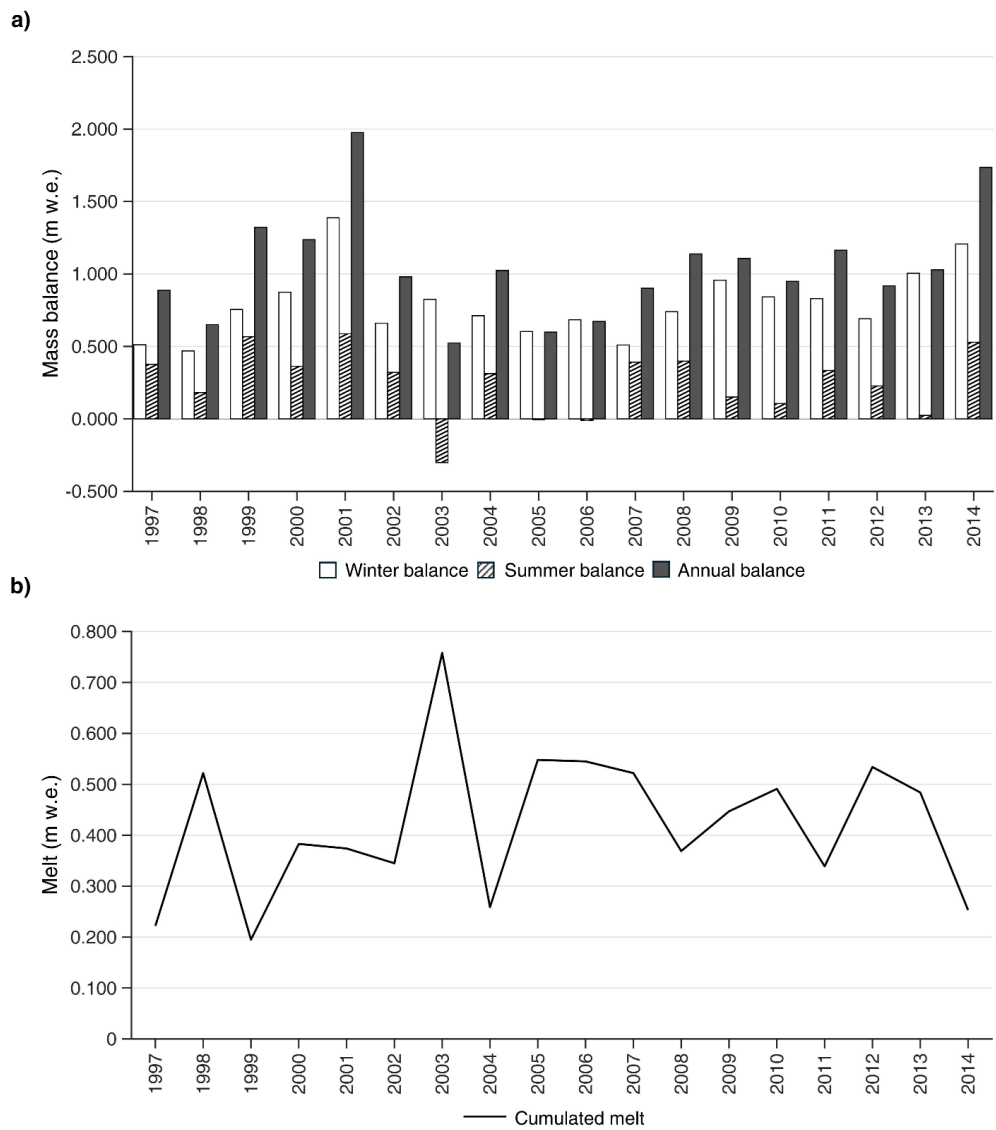
The interannual variability of mass balance was remarkable at both sites (Fig. 5). The annual balance was closely correlated with the winter balance (r = 0.80) and slightly less correlated with the summer balance (r = 0.78). The summer balance was +0.25 m w.e. on average, but was close to zero in 2005, 2006 and 2013, and negative only in 2003 (-0.30 m w.e.).

252   The total melt (Fig. 5b) was also highly variable from year to year, and ranged between 0.19 m w.e. in 1999 and 0.76 m

253   w.e. in 2003. A few phases of intense and prolonged melt in 2003, 2005, 2006, 2009, 2013 and 2010 led to the removal

254   of snow layers accumulated over long periods (Fig. 4). According to EISModel calculations, the snow accumulated

255   between 17 November 2002 and 27 August 2003 (more than 9 months) was entirely melted during the 2003 European

256   heat wave. Five months of snow accumulation were removed in 2006 (from early April to early September), 4 months in

257   2005 (from early April to July), 3 months in 2013 (from May to early August), 3 months in 2009 (from June to August)

258   and 3 months in 2010 (from May to July).

259   The two years with best preservation of accumulated snow were 1999 and 2014, when melt was scarce (0.195 and 0.253

260   m w.e., respectively) and discontinuous. In these cases, melt removed only short periods of snow accumulation during

261   summer, without affecting the older layers underneath.

262

a)

b)

263

Figure 5: Interannual variability of a) seasonal and annual balance, and b) annual cumulated melt based on EISModel

265   calculation at the Ortles drilling site.

266

267   **4.3 The modelled pseudo proxy**

268   In the analysed period, the pseudo-proxy SLFT series calculated by EISModel shows high interannual variability in the

269   seasonality (i.e. the difference in SLFT between winter and summer) and in the accumulation of firn layers preserving a

270   paleoclimatic signal (Fig. 6).

271 According to the model, during the years 2009-2011 snow accumulation largely offset ablation in both winter and
272 summer, preserving a marked seasonality in the water stable isotopes signal, with a good amplitude. Much less winter
273 snow accumulated in the two years 2007 and 2008, as can be seen from the thinner grey bars in Fig. 6. This caused
274 narrower troughs in SLFT, especially for 2007, whose trough is also higher compared to the following years. This is due
275 to scarce snow accumulation in the coldest months of winter 2007.

276 In 2006, summer ablation was 30% larger than average and removed the snow deposited from April to August.
277 Nevertheless, a large seasonal variation in SLFT is preserved thanks to snow accumulation in the coldest part of winter
278 and in late summer. A very sharp transition between cold and warm SLFT is observable in 2006 because winter and
279 summer layers are in direct contact.   In 2005, the cold-season trough in SLFT is barely visible because snow accumulation
280 in winter was scarce and spring snow was almost completely removed by melt.

281 The year 2004 shows a marked seasonality and a well-defined winter trough (comparable to that of 2006) thanks to good
282 winter accumulation and low summer ablation (Fig. 5). The two years 2002 and 2003 look like a single year, because the
283 exceptionally warm summer 2003 completely removed the snow accumulated in the winter season 2002-'03. The winter
284 2003 SLFT trough is therefore entirely missing from the record, and the November 2002 layers are in direct contact with
285 those of late August 2003 (thin white band between the 2003 and 2004 cold-season grey bars in Fig. 6). This is important
286 when counting annual layers and establishing a chronology in the firn core (see discussion below). Winter snow
287 accumulation was almost absent in the hydrological year 2001-'02, causing the formation of a rather warm cold-season
288 trough in SLFT.

289 High snow accumulation and low summer melt occurred in the 1999, 2000 and 2001 balance years. 2001 was a record-
290 setting winter accumulation year in this geographic area (Armando et al., 2002), as can be seen by the width of the cold-
291 season grey bar in Fig. 6. Summer accumulation was also the highest in the analysed period (Fig. 5). In 1999, there was
292 high summer accumulation, combined with negligible ablation, thus making it the second highest summer balance of the
293 analysed period.

294 In 1998 and especially in 1997, the seasonal variation of SLFT declines due to the very low accumulation in the coldest
295 months (lowest winter balance of the entire series, Fig. 5) and to the removal of the 1997 summer snow layers caused by
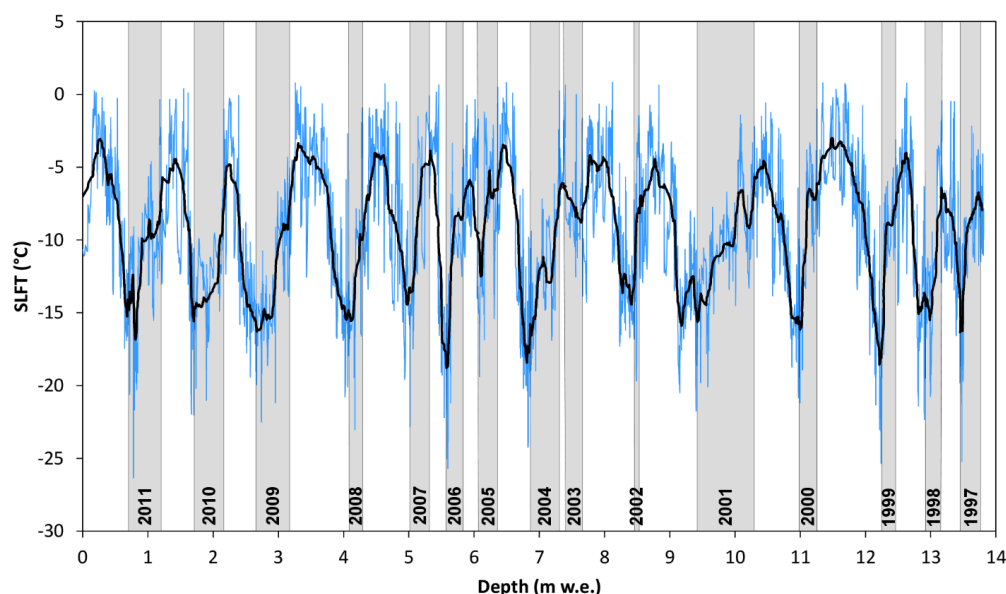296 an anomalous late-summer melt event, between August and September.

297

Figure 6: Snow layer formation temperature (SLFT) modelled at the drilling site by EISModel from September 1, 1996 to September 30, 2011. The black line is a 100-order centred moving average. The grey bars represent months from October to January (when pollen is not released, Fig. 7), in order to facilitate the following comparisons. The year is referred to the month of January (e.g., winter 1996-'97 is indicated as '1997').

302

4.4 Timescale based on pollen and stable isotopes

A tentative dating of the firn core extracted on Mt. Ortles was carried out based on annual layer counting based on stable isotopes and pollen measurements in the firn core (Fig. 7). We considered the depth interval from zero to 14 m w.e., the same as shown in Fig. 6. Winter layers were assigned based on troughs in the stable isotope series combined with very low/zero values in pollen concentration and PCA component scores (Section 3.2). Peaks in pollen concentration reflect the flowering season (Spring to Summer), while the lack of pollen indicates the non-flowering season (Autumn-Winter). Within each year, peaks in PC components indicate the presence of pollen types deriving from plant species blooming during spring, early summer and late summer (Festi et al., 2015 and 2017). This initial tentative timescale should represent 'routine' annual layer counting obtained using only experimental ice core data (like, for example, in Andersen et al., 2006; Takeuchi et al., 2019; Sinnl et al., 2022), independently from meteorological data or glacier mass balance observations or models.

The isotopic record is well preserved in the most recent four years (2011-2008) and is clearly smoothed by meltwater percolation before 2008, supporting the conclusions presented by Gabrielli et al. (2010). Stable isotope and pollen peaks match well within the firn layers. The pollen seasonality is well preserved for most years, except for 1999, 2006 and 2007, where the signals from spring, early summer, and late summer overlap. According to this initial tentative dating, the snow accumulation rate was larger before 2006 and smaller afterwards. When considering the layers with smoothed isotopes, there is a distinct peak that could initially be attributed to summer 2003; however, this is in clear contrast with EISModel

14

320 calculations, which indicate a complete ablation of the 2003 summer layers and removal of the associated isotopic signal

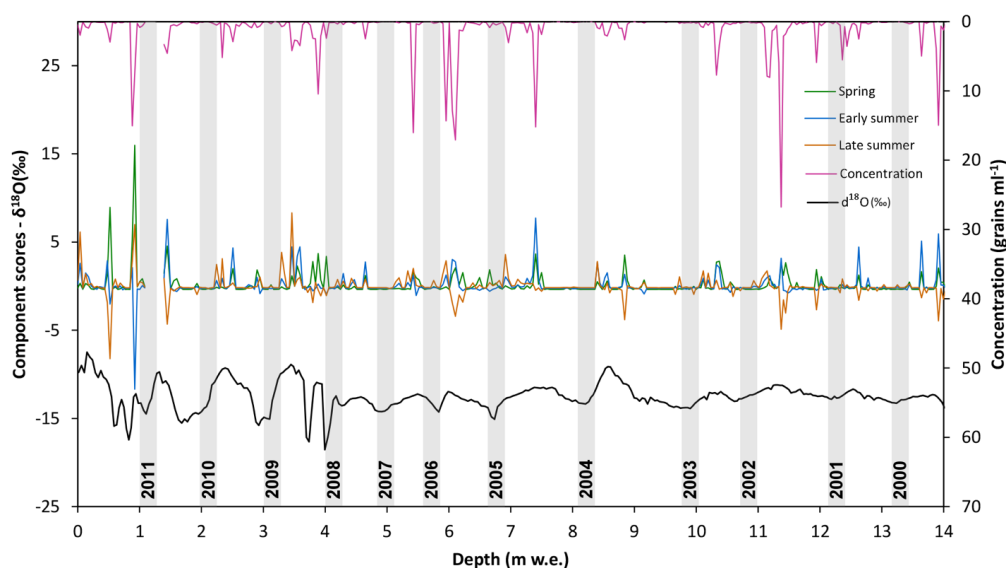321 (Section 4.3).

322

323

324 Figure 7: Concentration and principal component scores representative of spring, early summer and late summer of pollen

325 data extracted from the Mt. Ortles core 1, compared with the $\delta^{18}O$ values determined in the same core. Grey bars represent

326 mid-winter months (December and January) based on pollen data, and have arbitrary width. Annual layer counting is

327 based on $\delta^{18}O$ and pollen evidence.

328

4.5 Refined dating using the modelled pseudo proxy

330 A refinement of the tentative timescale in Fig. 7, based on the SLFT pseudo proxy modelled by EISModel, is presented

331 in Fig. 8. The annual layer counting from Fig. 7 matches the SLFT-based layer counting from 2011 to 2006. Below these

332 layers, we assigned the $\delta^{18}O$ trough at ~6.8 m w.e. depth to winter 2004 (instead of 2005) and considered the ~1 m w.e.

333 between 5.8 and 6.8 m as the result of two years of snow accumulation, 2004 and 2005. According to this interpretation,

334 the missing trough in the winter 2005 isotopic record is due to the low winter accumulation (Fig. 5a) and to the removal

335 of spring snow by ablation (Section 4.3, Fig. 6).

336 Similarly, we reinterpreted the $\delta^{18}O$ trough at ~8.2 m w.e. depth as winter 2002, whereas the winter trough of 2003 is

337 absent in the isotopic record because those winter layers completely melted during the 2003 warm summer. The annual

338 counting of firn layers below 2002 was consequently shifted according to these considerations, without other changes

339 compared to Fig. 7.

340 This reinterpretation (Fig. 8a) presents limited chronological discrepancies compared to the SLFT pseudo proxy (Fig. 8b),

341 without systematic under/overestimation of accumulation rates. These discrepancies would cancel each other over the

342 depth/period considered, as can be noted from the black lines that connect Figs. 8a and 8b, whose tilt seems randomly

343 distributed. Interestingly the major peak in isotopes at ~8.5 m w.e. depth dates summer 2001, instead of 2003 as attributed
344 merely on isotopes and pollen data (Section 4.4). This peak matches with the highest summer accumulation in the analysed
345 period (Fig. 5a; Armando et al., 2001). The second highest summer accumulation year (1999) matches with the secondary
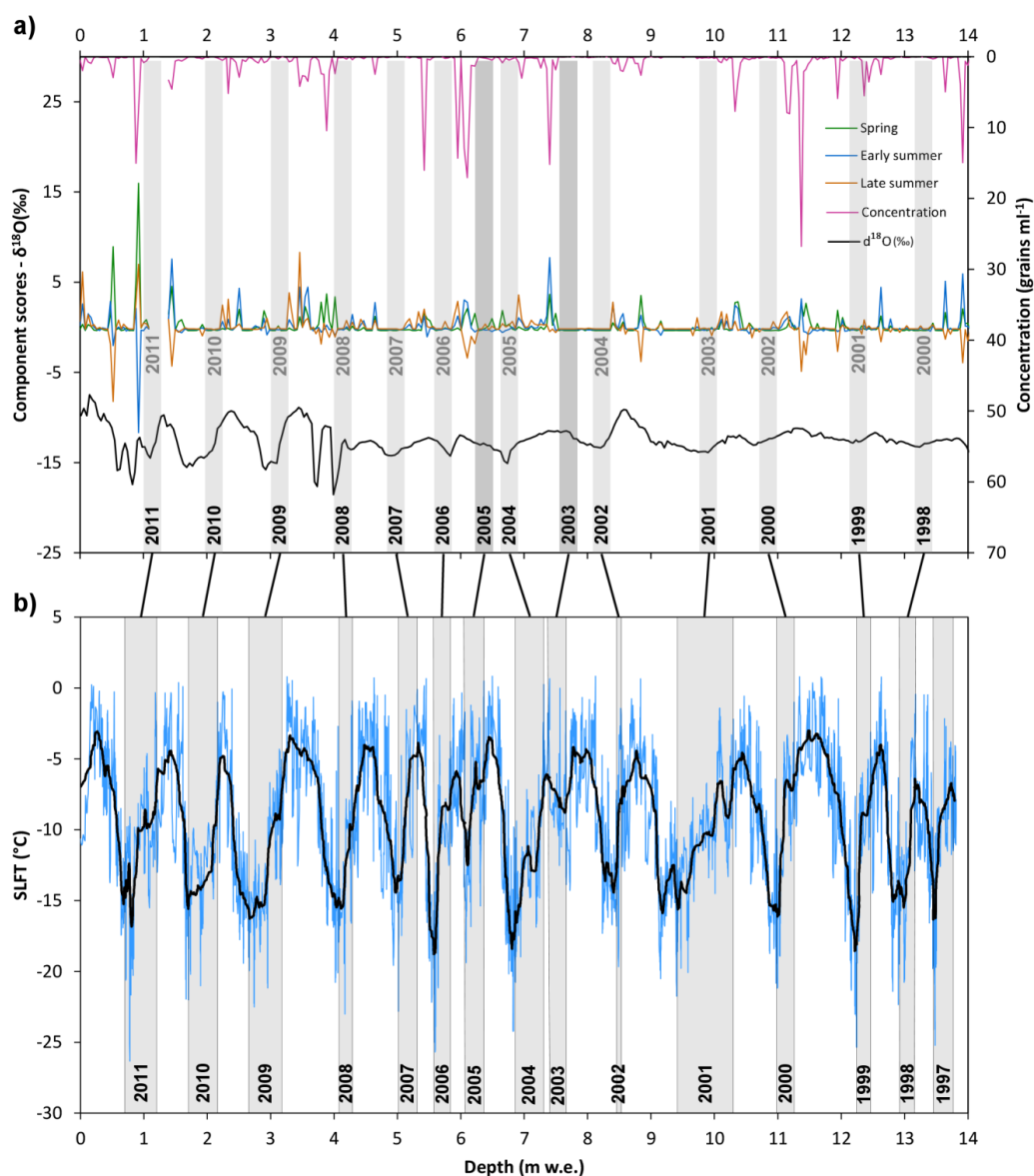346 peak in isotopes at ~11.5 m w.e. depth.

347

348

349 Figure 8: a) Same as Fig. 7 except annual layer counting reinterpreted based on b) snow layer formation temperature
350 (SLFT) modelled at the drilling site using EISModel. In a) the first timescale (shown in Fig. 7) is reported with a grey

351 font, to ease comparison. The two darker grey bars in a) indicate winter seasons that were missed in the timescale based

352 only on isotopes and pollen information, and added in the following using SLFT.

353

5 Discussion

355 The underlying assumption of our modelling approach is that the variability of local 2 m air temperature during snowfall

356 at the drilling site (i.e. the EISModel output variable SLFT) is representative of the $\delta^{18}O$ variability in snow deposited at

357 the same site. This is equivalent to assuming a linear relationship between 2 m air temperature and $\delta^{18}O$, whose variability

358 is affected by other processes such as the origin and history of the water vapour in the air mass, condensation cycles, sub-

359 cloud humidity, and preferential deposition and redistribution of snow by winds (Dansgaard, 1964; Sturm et al., 2010).

360 Another assumption is that the original $\delta^{18}O$ variability after snow deposition was preserved on Mt. Ortles, which in realty

361 is most likely modified by post depositional processes such as melt, sublimation, condensation, diffusion, isotopic

362 exchange between atmospheric water vapour and snow, and percolation of melt/rainwater (Eichler et al., 2001, Steen-

363 Larsen et al., 2014). All these effects may have caused a post-depositional increase in $\Box^{18}O$ values.

364 Because so many factors affect the original isotopic composition of snow and its variation through time, there are likely

365 limitations for our approach. However, the development of EISModel and of the pseudo proxy of snow temperature

366 formation were not intended to accurately reproduce the $\delta^{18}O$ variability measured in the ice cores retrieved on Mt. Ortles.

367 Instead, it was designed to be a tool to improve the interpretation of paleoclimatic data preserved in snow and firn cores,

368 particularly through more accurate firn annual layer counting. The modelling approach is based on scientific literature

369 supporting the main assumptions that i) ice cores contain temperature information that can be extracted from stable water

370 isotopes (e.g. Brönnimann et al., 2013; Hurley et al., 2016, Steiger et al., 2017) and ii) this temperature information and

371 its seasonal signature are preserved (although smoothed) after limited meltwater percolation (e.g. Moser et al., 2024).

372 However, completely melted layers cannot be represented in the retrieved stable isotope record, and the EISModel

373 specifically accounts for that.

374 The EISModel is an intermediate-complexity model aiming at representing the dominant processes affecting glacier mass

375 balance and paleoclimate proxy formation/preservation, while requiring only a few meteorological input data

376 (precipitation and air temperature). According to Evans et al. (2013), best-compromise models for paleoclimatic

377 applications are more complex than univariate-linear in their response to environmental forcings, without the need to

378 capture all fine-scale processes at play in a given proxy system.

379 At the Mt. Ortles drilling site, the two major processes that likely influence the formation and preservation of the isotopic

380 record are i) the seasonal distribution of precipitation/accumulation (taking into account the seasonal wind erosion) and

381 ii) the intensity and duration of summer ablation. Both show high interannual variability (Fig. 5), which is typical of the

382 climate of this region. Due to their importance and strong variability in time, they are explicitly modelled by EISModel

383 to build a pseudo proxy (SFLT) that can be helpful in studying ice core records retrieved at similar sites.

384 Overall, considering the model used and the characteristics of the study area, the model's skill in reproducing observed

385 mass balance is satisfying (Fig. 3) because the magnitude of RMSE values is comparable to the typical errors in mass

386 balance measurements (Zemp et al., 2013). A major simplification of our model is the use of a linear relationship between

387 accumulation and precipitation, meaning time-invariant vertical precipitation gradient and wind redistribution. This is

388   common in glacier mass balance models of similar complexity and is unavoidable without additional in-situ direct
389   observations of precipitation and snow redistribution.

390   The impact of this simplification is visible in the simulations of winter balance, which display a higher RMSE compared
391   to summer balance (Fig. 3). However, it must be considered that uncertainty and high spatial variability also affect winter
392   balance field measurements, not only simulations. Differences up to 0.5 m in snow depth above previous year's summer
393   surface were measured within soundings that were just 10 m apart. This is exacerbated by the difficulty of identifying the
394   summer surface in snow pits and snow depth soundings. However, since the RMSE does not exceed one third of the
395   annual snow accumulation rate, we are confident in the overall model's skill to discriminate between high and low
396   accumulation years/seasons.

397   Our approach share some similarities to that used by Brönnimann et al. (2013) who replicated the ice core from the
398   Grenzgletscher (Switzerland, 4200ma.s.l.) on a sample-by-sample basis by calculating precipitation-weighted
399   temperature (PWT) over short core intervals. However, this approach did not account for melt, whose effects are instead
400   explicitly calculated by our glacier mass balance model. Considering the increasing air temperature, melt events are
401   increasingly affecting high-altitude regions of temperate mountain areas, resulting in strong alterations of glacier mass
402   balance and vertical shift of dry-snow/percolation/wet-snow zones on glaciers. Besides deterioration of paleoclimatic
403   information contained in ice cores due to meltwater percolation, exceptional melt events can physically remove months
404   of snow accumulation from glaciers. This is happening at increasingly high elevation in the European Alps (Baroni et al.,
405   2023; Carrer et al., 2023) and is no longer limited to drilling sites below 4000 m a.s.l. (Huber et al., 2024). Even though
406   current melt rates are extremely high, similar intensity of melt might have occurred also in past epochs, for example
407   during the Holocene thermal maximum (Renssen et al., 2012; Kalis et al., 2003).

408   For these reasons, embedding a glacier mass balance model in proxy system models is a useful approach because of the
409   importance of ablation, together with accumulation, in determining how the climatic signal is recorded in the ice core
410   paleoclimatic records. Even though ablation may be assumed as negligible at an ice core drilling site at the present time
411   under the current climate, it might have been significant in the past, particularly at glacial-interglacial time scales.
412   Therefore, testing how melt events impact ice core records by means of glacier mass balance models embedded in proxy
413   system models can be useful for improved dating and interpretation of these paleoclimatic archives.

414   The SLFT pseudo-proxy clearly adds robustness to the firn core chronology, because it explicitly highlights the
415   interannual variability of snow accumulation and ablation. Nevertheless, the interpretation of some features in the stable
416   isotopes and pollen records remain uncertain. For example, the $\delta^{18}O$ peak at ~ 8.5 m w.e. (Figs. 7 and 8) is anomalous,
417   considering that the records from this section of the core were smoothed by melt water percolation. In Section 4.5 we
418   tentatively attributed this peak to the very high summer accumulation in 2001 (Fig. 5), but there might be alternative
419   explanations.

420   For instance, post-depositional effects due to the 2003 European heat wave could have caused an increase in $\delta^{18}O$ values
421   of the snow layers re-exposed during this extreme heat event, similarly to what has been observed for post depositional
422   changes of the isotopic composition of surface snow on the Greenland ice sheet (Steen-Larsen et al., 2014). In 2003, on
423   Mt. Ortles, the strong percolation of melt water might have relocated pollen grains (vertical and/or lateral drainage) thus
424   explaining the relative scarcity of pollen in the 2001 and 2002 layers in Fig. 8a.

425   The lack of a distinct peak in this section of the SLFT series, similar to the peak at ∼ 8.5 m w.e. observable in the δ18O

426   series, might suggest that the latter depends on post-depositional effects that are not considered in the ESIModel, like

427   sublimation, condensation, diffusion, and isotopic exchange between atmospheric water vapour and snow (Sokratov and

428   Golubev, 2009; Steen-Larsen et al., 2014; Ebner et al., 2017; Madsen et al., 2019).

429   As already discussed, the SLFT pseudo-proxy does not account for snow redistribution by wind, which is an important

430   process at this high-elevation site exposed to strong winds. According to snow depth observations on Mt. Ortles and

431   similar locations in this region (e.g., Fischer et al., 2022; Carturan et al., 2023) wind erosion strongly prevents snow

432   accumulation in the colder winter months, between January and March. For this reason, we think that further

433   improvements in the development of the pseudo proxy might be possible by including a simple parameterization of snow

434   erosion and its dependence on air temperature (Li and Pomeroy, 1997; He and Ohara, 2017).

435

436   **6 Conclusions**

437   In this paper, we present a model that simulates the mass balance history and reconstruct the glacier stratigraphy at the

438   Mt. Ortles ice core drilling site between 1996 and 2011. The model calculates the air temperature during the formation of

439   snow layers (SLFT). The SLFT is used as a pseudo proxy for improved dating and interpretation of the ice core

440   paleoclimatic archive retrieved on Mt. Ortles in 2011.

441   The model demonstrates good skill in reproducing the observed mass balance and proves to be useful for the interpretation

442   of the ice core data. It is particularly valuable in detecting two major ambiguities in annual layer counting based on stable

443   water isotopes and pollens, namely the two years 2005 and 2003, which lack a winter signal in the isotopic record. Without

444   the model reconstruction of the local mass balance, it would not have been possible to identify and quantify these two

445   anomalies, which stemmed from melt-induced removal of snow layers accumulated over several months or seasons.

446   Considering the current rate of atmospheric warming and the impact of extreme melt events (such as the warm 2003

447   summer in the European Alps), we suggest that modelling approaches accounting for accumulation and ablation processes

448   can be useful for understanding how the paleoclimatic signal is formed and preserved in ice cores.

449   These considerations may be valid for both the current warming phase and past climatic changes. Dating and interpretation

450   of ice core records formed during the Holocene thermal maximum, for example, may present issues similar to those

451   highlighted in this paper. During that period and perhaps in other warm phases of the Holocene (Renssen et al., 2012),

452   above-average summer melt, melting of large quantities of snow at the surface, and variations in snow drifting likely

453   occurred. Model-based studies similar to the one presented in this study can provide insights into these processes and can

454   enable detection of these events in past climate reconstructions based on ice cores, in particular those obtained near the

455   lower altitude limit for preserving atmospheric signals in snow and ice layers.

456

457   **Data availability**

458   Data are available from the corresponding author upon reasonable request.

459

References

Adler, S., Das Klima von Tirol-Südtirol-Belluno: 1981–2010; Vergangenheit-Gegenwart-Zukunft, Zentralanstalt für Meteorologie und Geodynamik; Südtirol Abteilung Brand- und Zivilschutz, Bozen, 102, 2015.

Andersen, K. K., Svensson, A., Johnsen, S. J., Rasmussen, S. O., Bigler, M., Röthlisberger, R., Ruth, U., Siggaard-Andersen, M. L., Peder Steffensen, J., Dahl-Jensen, D., Vinther, B. M., and Clausen, H. B.: The Greenland ice core chronology 2005, 15–42 ka. Part 1: constructing the time scale, Quaternary Sci. Rev., 25, 3246–3257, https://doi.org/10.1016/j.quascirev.2006.08.002, 2006.

494   Armando, E., Baroni, C., and Zanon, G.: Reports of the glaciological survey 2000. Relazioni della campagna glaciologica
495   2000, Geogr. Fis. e Din. Quat.,, 24(2), 203-261, 2001.

496   Baroni C., Bondesan, A., Carturan, L., Chiarle, M., and Scotti R.: Annual glaciological survey of Italian glaciers (2022)
497 | Campagna glaciologica annuale dei ghiacciai italiani (2022), Geogr. Fis. e Din. Quat.,, 46(1), 3-123,
498   https://doi.org/10.4454/gfdq.v46.883, 2023.

499   Bohleber, P.: Alpine Ice Cores as Climate and Environmental Archives. In P. Bohleber, Oxford Research Encyclopedia
500   of Climate Science. Oxford University Press, https://doi.org/10.1093/acrefore/9780190228620.013.743, 2019.

501   Bohleber, P., Schwikowski, M., Stocker-Waldhuber, M., Fang, L., and Fischer, A.: New glacier evidence for ice-free
502   summits during the life of the Tyrolean Iceman. Sci. Rep-UK, 10(1), 20513, https://doi.org/10.1038/s41598-020-77518-
503   9, 2020.

504   Bohleber, P., Wagenbach, D., Schöner, W., and Böhm, R.: To what extent do water isotope records from low
505   accumulation Alpine ice cores reproduce instrumental temperature series? Tellus B, 65(1), 20148,
506   https://doi.org/10.3402/tellusb.v65i0.20148, 2013.

507   Brönnimann, S., Mariani, I, Schwikowski, M., Auchmann, R., and Eichler, A.: Simulating the temperature and
508   precipitation signal in an Alpine ice core, Clim. Past, 9, 2013–2022, https://doi.org/10.5194/cp-9-2013-2013, 2013.

509   Carrer, M., Dibona, R., Prendin, A. L., and Brunetti, M.: Recent waning snowpack in the Alps is unprecedented in the
510   last six centuries, Nat. Clim. Chang., 13, 155–160, https://doi.org/10.1038/s41558-022-01575-3, 2023.

511   Carturan, L., Cazorzi, F., and Dalla Fontana, G.: Distributed mass-balance modelling on two neighbouring glaciers in
512   Ortles-Cevedale, Italy, from 2004 to 2009, J. Glaciol., 58(209), 467-486, https://doi.org/10.3189/2012JoG11J111, 2012a.

513   Carturan L., Dalla Fontana, G., and Borga, M.: Estimation of winter precipitation in a high-altitude catchment of the
514   Eastern Italian Alps: validation by means of glacier mass balance observations, Geogr. Fis. e Din. Quat., 35, 37-48,
515   https://doi.org/10.4461/GFDQ.2012.35.4, 2012b.

516   Carturan, L., De Blasi, F., Dinale, R., Dragà, G., Gabrielli, P., Mair, V., Seppi, R., Tonidandel, D., Zanoner, T., Zendrini,
517   T. L., and Dalla Fontana, G.: Modern air, englacial and permafrost temperatures at high altitude on Mt Ortles
518   (3905 m a.s.l.), in the eastern European Alps, Earth Syst. Sci. Data, 15, 4661–4688, https://doi.org/10.5194/essd-15-4661-
519   2023, 2023.

520   Cazorzi, F., and Dalla Fontana, G.: Snowmelt modelling by combining air temperature and a distributed radiation index.
521   J. Hydrol., 181(1–4), 169–187, https://doi.org/10.1016/0022-1694(95)02913-3, 1996.

522   Dansgaard, W.: Stable isotopes in precipitation, Tellus, XVI, 436–468, 1964.

523   Dietermann, N., and Weiler, M.: Spatial distribution of stable water isotopes in alpine snow cover, Hydrol. Earth. Syst.
524   Sc., 17(7), 2657–2668, https://doi.org/10.5194/hess-17-2657-2013, 2013.

525   Ebner, P. P., Steen-Larsen, H., Stenni, B., Schneebeli, M., and Steinfeld, A.: Experimental Observation of Transient δ18O
526   Interaction between Snow and Advective Airflow under Various Temperature Gradient Conditions, The Cryosphere, 11,
527   1733–1743, https://doi.org/10.5194/tc-11-1733-2017, 2017.

528 Eichler, A., Schwikowski, M., Gäggeler, H. W., Furrer, V., Synal, H.-A., Beer, J., Saurer, M., and Funk, M.:
529 Glaciochemical dating of an ice core from the upper Grenzgletscher (4200ma.s.l.), J. Glaciol., 46, 507–515,
530 https://doi.org/10.3189/172756500781833098, 2000.

531 Eichler, A., Schwikowski, M., and Gäggeler, H. W.: Meltwater-induced relocation of chemical species in Alpine firn,
532 Tellus B, 53, 192–203, https://doi.org/10.3402/tellusb.v53i2.16575, 2001.

533 Ekaykin, A. A. and Lipenkov, V. Y.: Formation of the ice core isotopic composition, Physics of ice core records, Low
534 Temp. Sci., 68, 299–314, 2009.

535 Erdtman, G.: The acetolysis method. A revised description. Svensk Bot. Tidskr., 54, 561–569, 1960.

536 Evans, M. N., Tolwinski-Ward, S. E., Thompson, D. M., and Anchukaitis, K. J.: Applications of proxy system modeling
537 in high resolution paleoclimatology, Quaternary Sci. Rev., 76, 16-28, https://doi.org/10.1016/j.quascirev.2013.05.024,
538 2013.

539 Faegri, K., Iversen, J., Kaland, P. E., and Krzywinski, K.: Bestimmungsschlüssel für die nordwesteuropäische Pollenflora.
540 Gustav Fischer, Jena, 1993.

541 Festi, D., Carturan, L., Kofler, W., dalla Fontana, G., de Blasi, F., Cazorzi, F., Bucher, E., Mair, V., Gabrielli, P., and
542 Oeggl, K.: Linking pollen deposition and snow accumulation on the Alto dell'Ortles glacier (South Tyrol, Italy) for sub-
543 seasonal dating of a firn temperate core, The Cryosphere, 11, 937–948, https://doi.org/10.5194/tc-11-937-2017, 2017.

544 Festi, D., Kofler, W., Bucher, E., Carturan, L., Mair, V., Gabrielli, P., and Oeggl, K.: A novel pollen-based method to
545 detect seasonality in ice cores: a case study from the Ortles glacier, South Tyrol, Italy, J. Glaciol., 61, 815–824,
546 doi:10.3189/2015JoG14J236, 2015.

547 Festi, D., Schwikowski, M., Maggi, V., Oeggl, K., and Jenk, T. M.: Significant mass loss in the accumulation area of the
548 Adamello glacier indicated by the chronology of a 46m ice core, The Cryosphere, 15, 4135–4143,
549 https://doi.org/10.5194/tc-15-4135-2021, 2021.

550 Fischer, A., Stocker-Waldhuber, M., Frey, M., and Bohleber, P.: Contemporary mass balance on a cold Eastern Alpine
551 ice cap as a potential link to the Holocene climate. Sci Rep 12, 1331, https://doi.org/10.1038/s41598-021-04699-2, 2022.

552 Gabrielli, P., Carturan, L., Gabrieli, J., Dinale, R., Krainer, K., Hausmann, H., Davis, M., Zagorodnov, V., Seppi, R.,
553 Barbante, C., Fontana, G. D., and Thompson, L. G.: Atmospheric warming threatens the untapped glacial archive of
554 Ortles mountain, South Tyrol, J. Glaciol,, 56, 843–853, https://doi.org/10.3189/002214310794457263, 2010.

555 Gabrielli, P., Barbante, C., Bertagna, G., Bertó, M., Binder, D., Carton, A., Carturan, L., Cazorzi, F., Cozzi, G., Dalla
556 Fontana, G., Davis, M., De Blasi, F., Dinale, R., Dragà, G., Dreossi, G., Festi, D., Frezzotti, M., Gabrieli, J., Galos, S. P.,
557 Ginot, P., Heidenwolf, P., Jenk, T. M., Kehrwald, N., Kenny, D., Magand, O., Mair, V., Mikhalenko, V., Lin, P. N.,
558 Oeggl, K., Piffer, G., Rinaldi, M., Schotterer, U., Schwikowski, M., Seppi, R., Spolaor, A., Stenni, B., Tonidandel, D.,
559 Uglietti, C., Zagorodnov, V., Zanoner, T., and Zennaro, P.: Age of the Mt. Ortles ice cores, the Tyrolean Iceman and
560 glaciation of the highest summit of South Tyrol since the Northern Hemisphere Climatic Optimum, The Cryosphere, 10,
561 2779–2797, doi:10.5194/tc-10-2779-2016, 2016.

562 Gabrielli, P., Barbante, C., Carturan, L., Cozzi, G., Dalla Fontana, G., Dinale, R., Draga, G., Gabrieli, J., Kehrwald, N.,
563 Mair, V., Mikhalenko, V. N., Piffer, G., Rinaldi, M., Seppi, R., Spolaor, A., Thompson, L. G., and Tonidandel, D.:
564 Discovery of cold ice in a new drilling site in the Eastern European Alps, Geogr. Fis. Dinam. Quat., 35, 101–105,
565 doi:10.4461/GFDQ.2012.35.10, 2012

566 García-Herrera, R., Díaz, J., Trigo, R. M., Luterbacher, J., and Fischer, E. M.: A Review of the European Summer Heat
567 Wave of 2003, Crit. Rev. Env. Sci. Tec., 40(4), 267–306. https://doi.org/10.1080/10643380802238137, 2010.

568 Haeberli, W., and Alean, J.: Temperature and accumulation of high altitude firn in the Alps, Ann. Glaciol., 6, 161-163,
569 https://doi.org/10.3189/1985AoG6-1-161-163, 1985.

570 Hashimoto, S., Zhou, S., Nakawo, M., Shimizu, M., and Ishikawa, N.: Temporal isotope changes in wet snow layers in
571 association with mass exchange between snow particles and liquid water in between the particles, Ann. Glaciol., 40, 128–
572 132, https://doi.org/10.3189/172756405781813492, 2005.

573 Hurley, J. V., M. Vuille, and D. R. Hardy (2016), Forward modeling of $\delta 18O$ in Andean ice cores, Geophys. Res. Lett.,
574 43, 8178–8188, https://doi.org/10.1002/2016GL070150, 2005.

575 He, S., and Ohara, N.: A new formula for estimating the threshold wind speed for snow movement, J. Adv. Model. Earth.
576 Sy., 9, 2514–2525. https://doi.org/10.1002/2017MS000982, 2017.

577 Horita, J., Ueda, A., Mizukami, K., and Takatori, I.: Automatic δD and $\delta 18O$ analyses of multi-water samples using H2–
578 and CO2–water equilibration methods with a common equilibration set-up, Appl. Radiat. Isot., 40, 801–805,
579 https://doi.org/10.1016/0883-2889(89)90100-7, 1989.

580 Huber, C. J., Eichler, A., Mattea, E., Brütsch, S., Jenk, T. M., Gabrieli, J., Barbante, C., and Schwikowski, M.: High-
581 altitude glacier archives lost due to climate change-related melting, Nat. Geosci., 17(2), 110–113.
582 https://doi.org/10.1038/s41561-023-01366-1, 2024.

583 Hurley, J. V., Vuille, M., and Hardy, D. R.: Forward modeling of $\delta 18O$ in Andean ice cores, Geophys. Res. Lett., 43,
584 8178–8188, https://doi.org/10.1002/2016GL070150, 2016.

585 Kalis, A. J., Merkt, J., and Wunderlich, J.: Environmental changes during the Holocene climatic optimum in central
586 Europe-human impact and natural causes. Quat. Sci. Rev., 22(1), 33-79, https://doi.org/10.1016/S0277-3791(02)00181-
587 6, 2003.

588 Laepple, T., Münch, T., Casado, M., Hoerhold, M., Landais, A., and Kipfstuhl, S.: On the similarity and apparent cycles
589 of isotopic variations in East Antarctic snow pits, The Cryosphere, 12, 169–187, https://doi.org/10.5194/tc-12-169-2018,
590 2018.

591 Lee, J.: A numerical study of isotopic evolution of a seasonal snowpack and its meltwater by melting rates, Geosci. J.,
592 18(4), 503–510. https://doi.org/10.1007/s12303-014-0019-5, 2014.

593 Li, L., and J. W. Pomeroy.: Estimates of Threshold Wind Speeds for Snow Transport Using eteorological Data, J. Appl.
594 Meteor. Climatol., 36, 205–213, https://doi.org/10.1175/1520-0450(1997)036<0205:EOTWSF>2.0.CO;2, 1997.

595 Madsen, M. V., Steen-Larsen, H. C., Hörhold, M., Box, J., Berben, S. M. P., Capron, E., Faber, A. K., Hubbard, A.,
596 Jensen, M. F., Jones, T. R., Kipfstuhl, S., Koldtoft, I., Pillar, H. R., Vaughn, B. H., Vladimirova, D., and Dahl-Jensen, D.:

597 Evidence of isotopic fractionation during vapor exchange between the atmosphere and the snow surface in Greenland, J.

598 Geophys. Res. Atmosperes, 124, 2932–2945, https://doi.org/10.1029/2018JD029619, 2019.

599 Moran, T., Marshall, S. J., and Sharp, M. J.: Isotope thermometry in melt-affected ice cores: ISOTOPE

600 THERMOMETRY. J. Geophys. Res.-Earth, 116(F2), https://doi.org/10.1029/2010JF001738, 2011.

601 Moser, D. E., Thomas, E. R., Nehrbass-Ahles, C., Eichler, A., and Wolff, E.: Review article: Melt-affected ice cores for

602 polar research in a warming world, The Cryosphere, 18, 2691–2718, https://doi.org/10.5194/tc-18-2691-2024, 2024.

603 Nakazawa, F., Fujita, K., Takeuchi, N., Fujiki, T., Uetake, J., Aizen, V., and Nakawo, M.: Dating of seasonal snow/firn

604 accumulation layers using pollen analysis, J. Glaciol., 51(174), 483–490, https://doi.org/10.3189/172756505781829179,

605 2005.

606 Neff, P. D., Steig, E. J., Clark, D. H., McConnell, J. R., Pettit, E. C., and Menounos, B.: Ice-core net snow accumulation

607 and seasonal snow chemistry at a temperate-glacier site: Mount Waddington, southwest British Columbia, Canada., J.

608 Glaciol., *58*(212), 1165–1175, https://doi.org/10.3189/2012JoG12J078, 2012.

609 Nye, J. F.: Correction factor for accumulation measured by the thickness of the annual layers in an ice sheet, J. Glaciol.,

610 4, 785–788, https://doi.org/10.3189/S0022143000028367, 1963.

611 Okazaki, A. and Yoshimura, K.: Global evaluation of proxy system models for stable water isotopes with realistic

612 atmospheric forcing, J. Geophys. Res.-Atmos., 124, 8972–8993, https://doi.org/10.1029/2018JD029463, 2019.

613 Pavlova, P. A., Jenk, T. M., Schmid, P., Bogdal, C., Steinlin, C., and Schwikowski, M.: Polychlorinated Biphenyls in a

614 Temperate Alpine Glacier: 1. Effect of Percolating Meltwater on their Distribution in Glacier Ice, Environ. Sci. Technol.,

615 49, 14085–14091, https://doi.org/10.1021/acs.est.5b03303, 2015.

616 Penna, D., Stenni, B., Sanda, M., Wrede, S., Bogaard, T.A., Michelini, M., Fischer, B.M.C., Gobbi, A., Mantese, N.,

617 Zuecco, G., Borga, M., Bonazza, M., Sobotkova, M., Cejkova, B., and Wassenaar, L.I.: Technical note: Evaluation of

618 between-sample memory effects in the analysis of δ2H and δ18O of water samples measured by laser spectroscopes,

619 Hydrol. Earth Syst. Sci. 16, 3925–3933, https://doi.org/10.5194/hess-16-3925-2012, 2012.

620 Renssen, H., Seppä, H., Crosta, X., Goosse, H., and Roche, D. M.: Global characterization of the Holocene thermal

621 maximum, Quat. Sci. Rev., 48, 7-19, https://doi.org/10.1016/j.quascirev.2012.05.022, 2012.

622 Sinnl, G., Winstrup, M., Erhardt, T., Cook, E., Jensen, C. M., Svensson, A., Vinther, B. M., Muscheler, R., and

623 Rasmussen, S. O.: A multi-ice-core, annual-layer-counted Greenland ice-core chronology for the last 3800 years:

624 GICC21, Clim. Past, 18, 1125–1150, https://doi.org/10.5194/cp-18-1125-2022, 2022.

625 Sokratov, S.A., and Golubev, V.N.: Snow isotopic content change by sublimation, J. Glaciol., 55, 823–828,

626 https://doi.org/10.3189/002214309790152456, 2009.

627 Steen-Larsen, H. C., Masson-Delmotte, V., Hirabayashi, M., Winkler, R., Satow, K., Prié, F., Bayou, N., Brun, E., Cuffey,

628 K. M., Dahl-Jensen, D., Dumont, M., Guillevic, M., Kipfstuhl, S., Landais, A., Popp, T., Risi, C., Steffen, K., Stenni, B.,

629 and Sveinbjörnsdottír, A. E.: What controls the isotopic composition of Greenland surface snow?, Clim. Past, *10*(1), 377–

630 392, https://doi.org/10.5194/cp-10-377-2014, 2014.

631 Steiger, N. J., Steig, E. J., Dee, S. G., Roe, G. H., and Hakim, G. J.: Climate reconstruction using data assimilation of
632 water isotope ratios from ice cores, J. Geophys. Res. Atmospheres, 122, 1545–1568,
633 https://doi.org/10.1002/2016JD026011, 2017.

634 Sturm, C., Zhang, Q., and Noone, D.: An introduction to stable water isotopes in climate models: benefits of forward
635 proxy modelling for paleoclimatology, Clim. Past, 6(1), 115-129, https://doi.org/10.5194/cp-6-115-2010, 2010.

636 Takeuchi, N., Sera, S., Fujita, K., Aizen, V. B., and Kubota, J.: Annual layer counting using pollen grains of the Grigoriev
637 ice core from the Tien Shan Mountains, central Asia, Arct. Antarct. Alp. Res., 51, 299–312,
638 https://doi.org/10.1080/15230430.2019.1638202, 2019.

639 Thompson, L. G., Davis, M. E., Mosley-Thompson, E., Porter, S. E., Corrales, G. V., Shuman, C. A., and Tucker, C. J.:
640 The impacts of warming on rapidly retreating high-altitude, low-latitude glaciers and ice core-derived climate records,
641 Global Planet. Change, 203, 103538, https://doi.org/10.1016/j.gloplacha.2021.103538, 2021.

642 Thompson, L. G., Mosley-Thompson, E., Davis, M. E., and Brecher, H. H.: Tropical glaciers, recorders and indicators of
643 climate change, are disappearing globally, Ann. Glaciol., 52(59), 23–34, https://doi.org/10.3189/17275641179909623,
644 2011.

645 Unnikrishna, P. V., McDonnell, J. J., and Kendall, C.: Isotope variations in a Sierra Nevada snowpack and their relation
646 to meltwater, J. Hydrol., 260(1–4), 38–57, https://doi.org/10.1016/S0022-1694(01)00596-0, 2002.

647 Zemp, M., Thibert, E., Huss, M., Stumm, D., Rolstad Denby, C., Nuth, C., Nussbaumer, S. U., Moholdt, G., Mercer, A.,
648 Mayer, C., Joerg, P. C., Jansson, P., Hynek, B., Fischer, A., Escher-Vetter, H., Elvehøy, H., and Andreassen, L. M.:
649 Reanalysing glacier mass balance measurement series, The Cryosphere, 7, 1227–1245, https://doi.org/10.5194/tc-7-1227-
650 2013, 2013.